An Enhanced Sensitivity of Alkanethiolate Self-Assembled Monolayers to Electron Irradiation through the Incorporation of a Sulfide Entity into the Alkyl Chains

K. Heister,[†] S. Frey,[†] A. Gölzhäuser,[†] A. Ulman,[‡] and M. Zharnikov*,[†]

Angewandte Physikalische Chemie, Universität Heidelberg, Im Neuenheimer Feld 253, 69120 Heidelberg, Germany, and Department of Chemistry and the NSF MRSEC for Polymers at Engineered Interfaces, Polytechnic University, Brooklyn, New York 11201

Received: June 18, 1999; In Final Form: October 7, 1999

A possibility to influence the response of self-assembled monolayers (SAM) of alkanethiolates (AT) to low-energy electron irradiation through the incorporation of specific molecular groups into the alkyl chains has been studied by using 11-(hexylmercapto)undecane-1-thiol (HMUT, $CH_3(CH_2)_5S(CH_2)_{11}SH$) SAM on gold substrate as a model system. In situ near-edge X-ray absorption fine structure spectroscopy and X-ray photoelectron spectroscopy (XPS) were applied as experimental tools. HMUT was found to form a dense, well-ordered self-assembled monolayer on Au with a coverage close to that of AT SAMs, a thickness of 19.8 ± 0.5 Å, and an average molecular tilt angle of 40° ± 2°. Features related to the thiolate and sulfide species could be easily distinguished in the S 2p XP spectra. Electron irradiation of the HMUT film gives rise to the same effects previously observed for AT SAMs such as disordering, partial dehydrogenation with C═C double bonds formation, desorption of the film fragments, reduction of the thiolate moieties, and the appearance of a new sulfur species. At the same time the extent of irradiation-induced desorption from the HMUT film is found to be noticeably larger (by ≈35%) than in AT SAMs, which is attributed to a higher sensitivity of the C−S bond to electron irradiation as compared to a C−C one. Some other differences with respect to AT SAMs such as sulfide-derived formation of C═S double bonds and a slightly reduced extent of irradiation-induced damage at the Au−alkanethiolate interface were also observed. The close resemblance of the binding energies of alkyl sulfide and the irradiation-induced sulfur species in AT SAMs implies an alternative assignment for the latter entities along with the commonly approved disulfide formation model, namely an incorporation of sulfur into the alkyl matrix via bonding to irradiation-induced carbon radicals in the adjacent aliphatic chains.

1. Introduction

Self-assembled monolayers (SAM), i.e., close-packed arrays of amphiphilic molecules in which the headgroup of an adsorbate covalently bonds to a substrate while the chainlike molecular tail sticks out from the substrate, have moved into the center of interest for scientists in physics, chemistry, and biology during the past two decades.[1] Because of their simple preparation, these systems provide a convenient way to form reproducible, well-ordered organic overlayers on a solid surface. The appropriate choice of the head and tail groups determines the strength of the bonding to the substrate and surface parameters like wetting, adhesion, lubrication, and corrosion. At the same time, the stability and the structure of SAMs are essentially influenced by the character of the molecule chain.

During the past years a strong scientific and technical interest concerning the response of SAMs toward ion, X-ray, UV, and electron irradiation has developed. One reason for this interest is the application of the related particles as spectroscopic primary tools for the characterization of SAMs, which can be accompanied by a partial damage of these systems through the respective irradiation.[2−4] Another issue is the possibility of a tailored SAM modification by the same primary sources within the lithography approach. The respective laterally modified SAM act then as a resist for wet chemical processing and reactive ion etching or as a chemical template for bonding of definite molecular groups.[5−8] The choice of suitable resists and optimal irradiation conditions requires an understanding of the precise character and extent of the irradiation-induced damage in different self-assembled organic layers.

At present such an understanding is in principle achieved only for the best investigated SAMs of alkanethiolates (AT).[2−4,9−11] These SAMs are composed of chainlike AT moieties anchoring to the suitable substrate through the thiolate headgroup.[1,12,13] The distance between the well-ordered alkyl chains forming a c(4×2) modulated $(\sqrt{3} \times \sqrt{3})R30°$ lateral lattice on Au(111) surfaces is about 4.97 Å, which corresponds to a lateral density of 4.65×10^{14} molecules/cm^2.[14,15] It has been shown that the X-ray[2,3] and electron[4,9−11,16] irradiation of AT SAMs results in a loss of orientational and conformational order and a dissociation of C−H, C−C, C−S, or S−Au bonds with a subsequent desorption of cut off fragments and the formation of new chemical bonds in the residual film such as C═C double bonds and S−S dimers, the latter molecular group probably serving as a precursor state for the subsequent desorption of sulfur-containing fragments. This behavior might be influenced by the modification of AT moieties through incorporation of specific functionalities, such as sulfur bridge groups. Following simple inelastic scattering consideration these functionalities are ex-

* To whom correspondence should be addressed. E-mail: o60@ix.urz.uni-heidelberg.de.
[†] Universität Heidelberg.
[‡] Polytechnic University, Brooklyn, NY.

10.1021/jp992017d CCC: $18.00
Published on Web 12/01/1999

pected to become predetermined breaking points due to the significantly lower bonding energy of the C−S bond (≈66 kcal/mol) as compared to that of a C−C bond (≈88 kcal/mol). Although these values are not a measure of the corresponding dissociation probabilities because the dissociation occurs in reality through irradiation-induced electron excitations, their large difference can be considered as an indication for an enlarged response of the modified AT SAMs to X-ray or electron irradiation. This would make sulfur bridge modified AT SAMs to a more sensitive lithographic resist as compared to the conventional AT films.

In the present study, the properties of SAMs formed from 11-(hexylmercapto)undecane-1-thiol (HMUT, $CH_3(CH_2)_5S-(CH_2)_{11}SH$) on gold substrate and their modification by low-energy electron irradiation are investigated. First, the structure of the HMUT monolayer is examined in order to determine the influence of the sulfide entity insertion on the AT monolayer characteristics. Second, the modification of the HMUT film by electrons with a primary energy of 10 eV is studied. Near-edge X-ray absorption fine structure (NEXAFS) spectroscopy and X-ray photoelectron spectroscopy (XPS) have been chosen as experimental tools. The combination of these techniques enables us to probe both the occupied and unoccupied states of an organic layer and to monitor its composition, spatial structure and chemical identity.

The data for HMUT/Au are compared with the results for two reference systems, dodecanethiolate $CH_3(CH_2)_{11}S^-$ (C12) and octadecanethiolate $CH_3(CH_2)_{17}S^-$ (C18) SAMs on gold, which are supposed to be similar to the HMUT film regarding the chemical composition and geometrical structure (the entire results for the reference systems are presented in ref 11). Such a comparison allows a simpler and more pictorial consideration of the HMUT/Au data.

In the following section the experimental procedure and techniques are shortly described. Thereafter, the results are presented and briefly discussed in section 3. A detailed analysis of the data is given in section 4 followed by a summary and suggestions for future research in section 5.

2. Experimental Section

The HMUT, C12, and C18 SAMs were prepared by 24 h immersion of Au substrates in the corresponding ethanolic solutions. The substrates consisted of 200 nm thick polycrystalline gold layer evaporated onto a titanium-primed (5 nm) Si(100) wafer (Silicon Sense). The concentrations of the HMUT and C12/C18 in the solutions were 0.5 and 1 mM, respectively. After the immersion the samples were rinsed with ethanol, blown dry by pure nitrogen, and stored in nitrogen atmosphere.

Both the pristine and irradiated HMUT films were characterized by NEXAFS spectroscopy and XPS in a modified multitechnique UHV chamber[17] attached to the HE-TGM 2 beamline[18] at the synchrotron radiation facility BESSY I in Berlin. The experiments were performed under UHV conditions (≈2×10^{-9} mbar) and at room temperature.

Electron irradiation was performed with a specially designed flood gun in the same vacuum chamber in which the XPS and NEXAFS measurements were carried out. The films were irradiated with electrons of a 10 eV energy and exposures of 300, 1000, 3000, and 8000 μC/cm^2, which correspond to ≈4.0, ≈13.5, ≈40, and ≈110 primary electrons per thiol molecule. The electron flux was ≈2.5 μA/cm^2 as estimated with the help of a Faraday cup. The flux stability during an irradiation cycle was controlled by the sample current.

The NEXAFS measurements were carried out at the C 1s absorption edge in the partial yield mode with a retarding voltage of −150 V. The incoming synchrotron radiation was linear polarized with the polarization factor of about 92%. The angle of light incidence was varied from 90° to 20° to monitor the average orientation of the HMUT, C12, and C18 molecules in the investigated SAMs. The corresponding approach is based on the dependence of the X-ray absorption cross section on the angle between the electric field vector and the molecular orbital involved in the photoexcitation process.[19] The acquisition time of a NEXAFS spectrum was about 4 min. The raw spectra were normalized to the incident photon flux by division through a spectrum of a clean, freshly sputtered gold sample. The absolute energy scale was set with the help of a NEXAFS spectrum of a graphite sample (HOPG) with a characteristic π^* resonance at 285.38 eV.[20] The individual NEXAFS spectra were calibrated to this scale by using a simultaneously recorded absorption spectrum of a carbon covered gold grid showing a characteristic resonance at about 285 eV.

The XPS measurements were carried out with a Mg Kα X-ray source ($E_{phot} = 1253.6$ eV) and a VG CLAM 2 spectrometer in normal emission geometry. The X-ray source was operated at 260 W power and positioned about 1−1.5 cm away from the samples. For both the pristine and irradiated films the Au 4f, wide scan, C 1s, O 1s, and S 2p spectra were measured. No contaminations were found. The energy resolution of the narrow scan spectra was about 0.9 eV, and the accuracy of the respective measurements was ≈0.05 eV. The binding energy scale was calibrated to the Au $4f_{7/2}$ peak at 84.0 eV.[21] To correct for possible deviations in the photon flux and sample position, the raw XP spectra were normalized to the integrated intensity of the wide scan spectra. This approach is reasonable because the vast majority of photoelectrons and secondary electrons originates from the Au substrate, which is common for all samples. An attenuation of the respective electrons by the relatively thin organic adlayer causes only a slight dependence of the total electron yield intensity on the SAM thickness.[22] The resulting XP spectra were fitted using a Shirley-type background[23] and symmetric Voigt profiles[24] consisting of variable Gauss and Lorentz components. To fit the S $2p_{3/2,1/2}$ doublet, we used a pair of Voigt peaks with the same width and Gauss/Lorentz proportion, the standard[21] spin−orbit splitting of 1.2 eV and the intensity ratio of 2 (S $2p_{3/2}$/S $2p_{1/2}$). The acquisition time of the XP spectra set was about 15 min, which was a compromise between acceptable statistics and low X-ray damage.

3. Results

NEXAFS experiments provide information about the occurrence and average orientation of the unoccupied molecular orbitals within the organic film of interest.[19] In Figure 1, C 1s NEXAFS spectra of a HMUT film (a) acquired at various X-ray incidence angles are presented in comparison with the respective C12 (b) and C18 (c) data. For all three systems the general shape of the absorption spectra is quite similar. The spectra are composed of the C 1s adsorption edge located at ≈288 eV,[25−27] and characteristic resonances at ≈288, ≈293, and ≈302 eV. The two latter resonances labeled C−C σ^* and C−C′ σ^* have been attributed to excitations into the antibonding C−C orbitals of the alkyl chains,[25,26] which are assumed to be oriented along the chain axis.[25,28,29] The orbitals related to the resonance at ≈288 eV are supposed to be oriented perpendicular to the alkyl chains[19,25,28,29] but the exact nature of this resonance is still under discussion. It was attributed to excitations into pure valence orbitals,[19] predominately Rydberg states[30] or mixed valence/

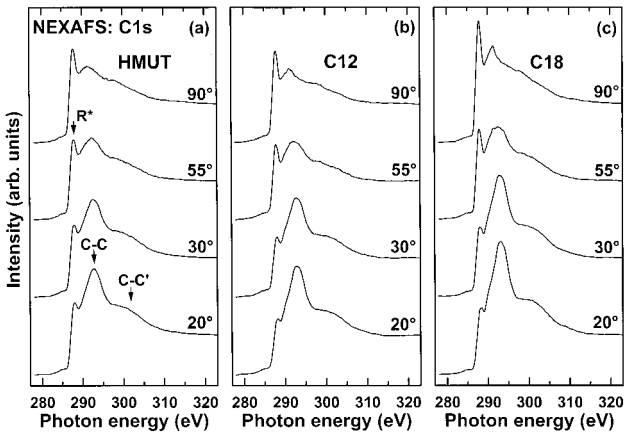

Figure 1. C 1s NEXAFS spectra of the pristine HMUT (a), C12 (b), and C18 (c) films at different angles of X-ray incidence. The positions of the characteristic NEXAFS resonances are indicated by arrows in (a).

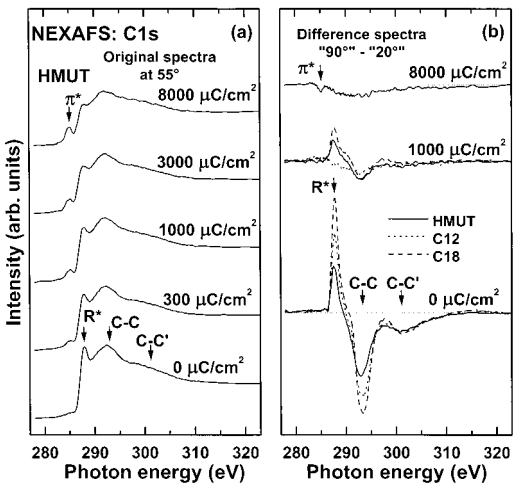

Figure 2. C 1s NEXAFS spectra recorded at an X-ray incident angle of 55° (a) and the differences of NEXAFS spectra acquired at X-ray incident angles of 90° and 20° (b) for the pristine (bottom curve in (a) and solid bottom curve in (b)) and irradiated HMUT films. The respective difference spectra for C12 (dotted line) and C18 (dashed line) are depicted in (b). The positions of the characteristic NEXAFS resonances and the respective anisotropy maxima are indicated by arrows.

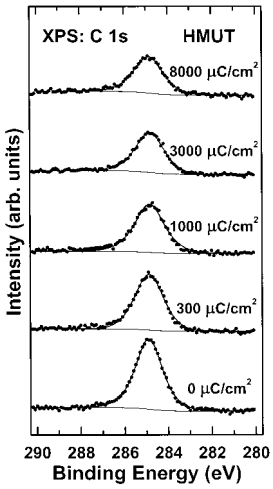

Figure 3. C 1s XP spectra for the pristine (bottom curve) and irradiated HMUT films.

Rydberg states.[31] We will denote this resonance as R* resonance but take into account a possible admixture of antibonding C−H* orbitals.

Among the spectra presented in Figure 1, the spectra acquired at the magic X-ray incidence angle of 55° exclusively reflect the electronic structure of the unoccupied molecular orbitals of the investigated films and are not affected by the angular dependence of the adsorption cross sections.[19] The comparison of the corresponding spectrum for HMUT/Au with those for C12 and C18 shows that the intensities of the R* and C−C σ* resonances for the former system are slightly lower than those for C12 and noticeably smaller than those for C18. Considering that all shown absorption spectra are normalized to the height of the C 1s absorption edge and, consequently, to the number of carbon atoms in the corresponding molecules, the observed difference can only be attributed to some intrinsic properties of the investigated systems. Generally, the excitation probabilities of the R* and C−C σ* resonances for AT SAMs are known to increase with the length of the intact alkyl chain,[11,25] which is probably related to the delocalization of the respective orbitals over the whole alkyl chain. The sulfide moiety built in the hydrocarbon tail evidently disturbs this assembly which consequently behaves as two separate chains consisting of only 6 and 11 methylene entities. This results in the excitation probabilities corresponding to short-chain AT SAMs, which explains the lower intensities of the R* and σ* resonances for HMUT as compared to those for C12 and C18 with 12 and 18 CH_2/CH_3 entities, respectively.

The average orientation of the alkyl chains can be estimated with the help of the linear dichroism of the C 1s NEXAFS spectra i.e., the dependence of the resonance intensities on the angle of light incidence. As a fingerprint of this effect a difference of the spectra acquired at incidence angles of 90° and 20° can be taken. The respective difference curves for the pristine HMUT, C12, and C18 films are depicted in the bottom graph of Figure 2b. The pronounced anisotropy peaks related to the R* and σ* resonances for HMUT/Au imply a good orientational order in this SAM. The anisotropy peaks have the same signs as those for C12 and C18 but smaller amplitudes. This implies a predominately vertical orientation of the HMUT molecules with an average molecular tilt angle exceeding that for the conventional AT SAMs (33°). The determination of the average orientation of the HMUT alkyl chains based on the linear dichroism of the R* resonance was performed via the difference spectra method[19] using the 90°−55°, 30°−55°, and 20°−55° difference spectra and the C12 sample as a reference system with a tilt angle of 33°.[11,25] The resulting average tilt angle of the HMUT alkyl chains with respect to the surface normal was found to be 42 ± 2°.

Complementary information is provided by XPS measurements. The C 1s and S 2p XP spectra of the pristine HMUT sample are shown in Figures 3 and 4a (bottom curves). In the C 1s spectrum a single peak at 284.9 eV with a full width at half-maximum (fwhm) of 1.42 eV is observed. The binding energy (BE) of this peak practically coincides with the respective value for the C18 reference sample implying similar polarizability of these systems.[32] The fwhm of the C 1s peak in HMUT/Au is somewhat higher than that value for AT SAMs (1.26 eV) reflecting a disturbance of the intact alkyl chain by the incorporated sulfide moiety.

Assuming an exponential attenuation of the photoelectrons originating from the Au substrate by the adlayer,[33] an effective film thickness of 19.8 ± 0.5 Å was obtained for the pristine HMUT film. A clean, sputtered Au sample was taken as a reference, and the attenuation length of the Au 4f photoelectrons with kinetic energy of ≈1170 eV was assumed to be 29.8 Å.[34,35]

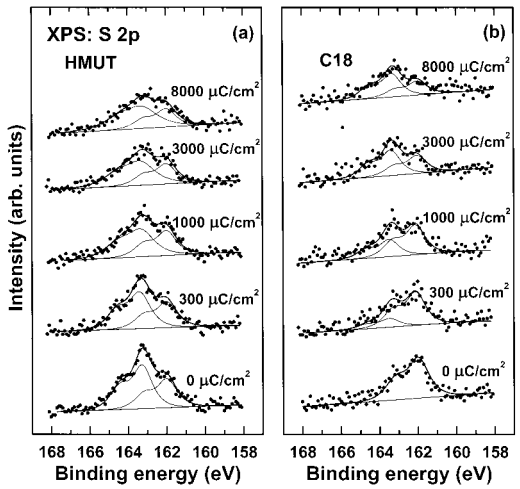

Figure 4. S 2p XP spectra for the pristine (bottom curves in (a) and (b)) and irradiated HMUT (a) and C18 (b) films. The S 2p emission structure is fitted by two doublets of Voigt peaks with fixed S $2p_{3/2}$/S $2p_{1/2}$ intensity ratio of 2 and energy separation of 1.2 eV (see text for a detailed explanation).

The found effective thickness provides an alternative way to determine the average tilt angle of the alkyl chains of the HMUT molecules in the respective SAM. Assuming the all-trans conformation of these molecules, a length of 1.27 Å per methylene unit,[36] Au−S and C−S bond lengths of 1.8[27] and 1.815 Å,[37] respectively, and a kink of 7.2° in the molecule axis around the sulfide unit as estimated by MM2 force field calculations,[38,39] we get an average tilt angle of ≈39° in a good agreement with the NEXAFS-derived value.

The S 2p XP spectrum of the pristine HMUT sample was deconvoluted into two S $2p_{3/2,1/2}$ doublets (see section 2) with the fwhm of the individual S $2p_{3/2}$ and S $2p_{1/2}$ peaks equal to 1.2 eV (the last value is predominately related to the energy resolution of our spectrometer and was derived from the spectrum of the pristine AT film which contains only one sulfur species). The respective S $2p_{3/2}$ peaks are located at 162.0 and 163.3 eV. The lower-BE doublet can be attributed to the thiolate-type headgroup while the higher-BE doublet can be related to the sulfide entity. These assignments are derived from the similarity of the related binding energies with the respective values for the conventional AT SAMs[2−4,40−44] (see also the bottom spectrum in Figure 4b) and 1,8-octanedithiol on gold,[44] respectively. A larger intensity of the higher-BE S 2p doublet as compared to the lower-BE one is related to the different signal attenuation by the covering organic layers. If corrected for this effect the intensities of both doublets practically coincide with each other as expected for the HMUT molecule. These intensities can also be compared with the respective value for the conventional AT SAMs, which gives an estimate for the thiolate signal in HMUT/Au to be ≈96% of the C18 one. Hence the coverage of the HMUT and C18 films is quite similar.

We now turn to the effect of low-energy (10 eV) electron irradiation on the HMUT SAM. The C 1s NEXAFS spectra of the irradiated HMUT, C12, and C18 films acquired at an X-ray incident angle of 55° and the differences of the respective spectra taken at incident angles of 90° and 20° are depicted in Figure 2, a and b. As is seen from Figure 2, the electron bombardment results in noticeable changes in both the NEXAFS spectra and the difference curves, the changes being in general similar to those in the conventional AT SAMs.[4,10,11] The intensities of the R*− and C−C-/C−C′− σ* resonances and the amplitudes of the respective anisotropy maxima in the difference curves decrease in the course of the irradiation and a new feature (π*-resonance) at ≈285 eV characteristic for C═C double bonds appears (a very small maximum observed at this energy for pristine AT SAMs is commonly related to a small amount of contamination[45] or excitation into alkane−metal orbitals[46]). As was shown previously,[4,10,11] this development can be attributed to decrease and disappearance of the orientational and conformational order, the pronounced desorption of hydrogen and carbon-containing fragments, and the appearance of C═C double bonds in the irradiated HMUT film. Some of these processes seem, however, to occur with slightly lower rates than in conventional ATs. In particular, the amplitudes of the anisotropy maxima in the difference curves for HMUT, C12 and C18 in Figure 2b become very similar after an irradiation of these films with a dose of 1000 μC/cm^2, whereas the respective amplitudes for the pristine HMUT film are significantly smaller than those for C12 and C18 (dotted and dashed curves, respectively). Another difference of the irradiation induced damage in the HMUT film as compared to the conventional AT SAMs is the appearance of the double π*-resonance structure around ≈285 eV in the former film instead of a single π*-resonance observed in the latter systems. The additional π*-resonance in the HMUT film can be possibly related to the formation of C═S double bonds (thiocarbonyls). This may result from the loss of hydrogen from a CH_2 α and subsequent double bonding of the residual CH moiety to an irradiation-induced S radical:

$$-CH_2-S^{\bullet} \rightarrow -CH{=}S + H^{\bullet}$$

The S radicals can result from an irradiation-induced desorption of the carbon-containing fragments in the HMUT film. Following the XPS data, this process is noticeably stronger in HMUT than in the conventional AT SAMs: The intensity of the C 1s peak in HMUT shows a decrease by 45% of its initial value (Figure 3) after irradiation with a dose of 8000 μC/cm^2, whereas the respective reduction for C18 layers is only 20%. The desorption processes result in a significant thickness reduction as shown in Figure 5a where the effective thickness reductions of the HMUT, C12, and C18 films (solid, dashed, and dotted curves, respectively) estimated through the analysis of the Au 4f XP intensity[33] are depicted as functions of the delivered dose. In all three systems the initially fast thickness reduction levels off at higher doses and reaches saturation values of −8.2 and −6.1 Å in the HMUT and C12/C18 films, respectively. The deviation in the HMUT thickness reduction from the curves obtained for the ATs develops already within the initial stages of the irradiation.

Both sulfur species in the HMUT film are affected by electron irradiation. The corresponding S 2p XP spectra in comparison with those for the C18 reference film are shown in Figure 4, a and b, respectively. To decompose these spectra into the contributions related to the individual sulfur species we consistently tried to fit the both spectra series by two S 2p doublets (see section 2). In the case of C18 we have succeeded in fitting all spectra in Figure 4b by varying only the intensities of the thiolate- and "irradiation"-related doublets from spectrum to spectrum and keeping the widths (1.2 eV for both the S $2p_{3/2}$ and S $2p_{1/2}$ peaks) and the energy positions of these doublets fixed for the complete spectra set. Extending the joint energy positions and width of the individual S $2p_{3/2}$ and S $2p_{1/2}$ peaks to the S 2p spectra for the HMUT films, we have only succeeded in fitting the spectrum for the pristine SAM as was described above. For the irradiated HMUT films the procedure only worked if the width of the S $2p_{2/3,1/2}$ peaks of the higher BE doublet was increased up to 2 eV which implies that in reality this fit structure consist of several S 2p doublets related to the

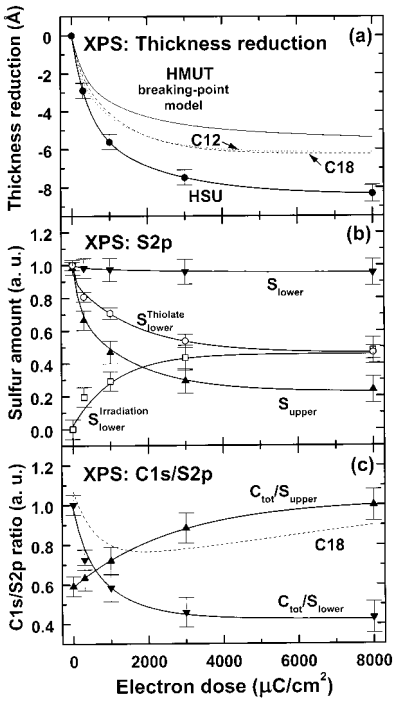

Figure 5. Evaluation of the irradiation-induced damage in the HMUT film: (a) effective thickness reduction of the HMUT film (filled circles and solid line), (b) normalized amounts of the sulfur species in the lower (filled down triangles) and upper (filled up triangles) sulfur levels as well as the normalized amounts of the thiolate (open circles) and irradiation-induced sulfur species (open squares) in the latter level, (c) normalized ratios of the C 1s XPS intensity to the S 2p intensities related to the lower (filled down triangles) and upper (filled up triangles) sulfur levels. In (a) and (c) the respective curves for C12 (dotted line) and C18 (dashed line) are also shown. The expected thickness reduction in the case that only C−S bond is breaking is depicted in (a) as thin solid line. The C_{tot}/S_{upper} curve in (c) is normalized to the value at 8000 μC/cm^2.

different sulfur species. Considering the small energy separation of these assumed doublets, we did not try to decompose the fit higher BE doublet any more but considered this feature as a whole.

As viewed in Figure 4a the intensities of both the higher and lower binding energy doublets in the S 2p spectra for HMUT/Au clearly decrease in the course of electron irradiation. The decrease of the latter doublet is known[2−4,11] to be related to both the desorption of thiolate-containing fragments and the transformation of thiolate in a new irradiation-induced sulfur species with the S $2p_{3/2}$ BE of ≈163.3 eV (see also Figure 4b), which practically coincides with that for the sulfide in the pristine HMUT film. The respective S 2p doublet should therefore appear at this BE and increase in intensity with the progressive irradiation as it happens in AT SAMs. In the HMUT film this process competes, however, with the decrease of the identically located sulfide-related doublet due to desorption of sulfide-containing fragments. In addition, a transformation of the pristine sulfide into other sulfur species can occur. Considering the enlarged (as compared to AT SAMs) value of the respective S $2p_{3/2,1/2}$ peak fwhm (see above), some of these species have to differ from the irradiation-induced sulfur species of AT SAMs. Taking into account the NEXAFS results, the additional, irradiation-induced sulfur species in HMUT SAM can be presumably assigned to sulfur atoms involved into C═S double bonding.

4. Discussion

The presented NEXAFS and XPS results provide information about the geometric, chemical, and electronic structure of the HMUT monolayer. The data shown in Figure 1 and the bottom graphs of Figures 2, 3, and 4 imply an HMUT self-assembly in a dense, well-ordered array of tilted molecules bond to the substrate via a thiolate-gold bond. The coverage of the gold substrate by HMUT molecules reaches ≈96% of the C18 value. The values of the average molecular tilt angle of ≈40°, independently obtained from the analysis of the NEXAFS and XPS data, agree well with each other. The layer thickness is 19.8 Å.

Electron irradiation has a strong effect on the HMUT SAM. A significant reduction of the orientational and conformational order in this system is exhibited by a decrease of the intensity and the linear dichroism of the NEXAFS resonances (Figure 2b). The decrease of the R* resonance and the growth of the π^* resonance at 285.0 eV imply a dehydrogenation and formation of C═C double bonds within the HMUT film. The desorption of carbon-containing fragments accompanied by a thickness reduction is also observed, the reduction being ≈35% larger for HMUT as compared to ATs. Note that the thickness derived from the XPS data resembles the layer thickness given by the occurrence of a definite amount of substance. A SAM compression related to its disordering does not influence the intensities of XP peaks.[4]

The enhanced sensitivity of HMUT/Au to electron irradiation as compared to ATs must be related to the incorporated sulfur. The behavior of this entity should be, therefore, considered in detail which was done using the intensities of the individual S 2p doublets derived from the S 2p spectra in Figure 4a. The error bars of these values are predominately related to the relatively low signal/noise (S/N) ratio of the S 2p spectra which stems from the limited time of the spectroscopic characterization (see section 2). The positions of the doublets and the widths of the individual S $2p_{3/2}$ and S $2p_{1/2}$ peaks were determined within the self-consistent analysis of the entire spectra series for both the C18 and HMUT films (see section 3).

As was mentioned above, the higher-BE S 2p doublet in Figure 4a contains contributions related to both the pristine sulfide and an irradiation induced sulfur species originating from both pristine sulfide and thiolate. The amount of thiolate species can be evaluated based on the reduction of the lower-BE S 2p doublet. A partial desorption of the thiolate-derived species can also be taken into account, assuming the portions of desorbed and remaining thiolate-derived, irradiation-induced species to be the same as for C18 SAM.

This procedure was applied to all spectra in Figure 4a. The amount of the sulfide-related species was obtained by the subtraction of the thiolate-related contribution in the higher-BE S 2p doublet. The different attenuation of the thiolate-related signal as compared to the sulfide-derived one (the respective species are covered by a thinner hydrocarbon layer or placed on the film surface for strongly irradiated films) was taken into account. The resulting amounts of the different sulfur species corrected for the respective attenuation by the covering hydrocarbon layers are shown in Figure 5b. To distinguish between the sulfide- and thiolate-related species we use the terms "upper" and "lower" sulfur level, respectively. For the lower level the total amount of the sulfur species $S_{lower} = S_{thiolate} + S_{irradiation}$ decreases very slowly with the progressive electron irradiation and reaches 95% of its initial value at 8000 μC/cm^2. The portion of the thiolate entities $S_{thiolate}$ decreases exponentially to 47% of its initial amount while $S_{irradiation}$ increases exponentially and

achieves ≈46% of $S_{thiolate}$ for the pristine HMUT film. Compared with the conventional AT SAMs, this transformation of thiolate into the irradiation-induced species occurs noticeably slower. In particular, the amount of the latter species in C18 exceeds that of thiolate already after irradiation with a dose of ≈1500 $\mu C/cm^2$ and finally reaches ≈57% of the initial thiolate amount whereas only 28% of the thiolate species survive.

The amount of sulfur in the upper level in HMUT/Au decreases exponentially in the course of irradiation and levels off at ≈22% of the initial amount. Thus, almost 80% of the sulfide species desorb along with the respective $CH_3(CH_2)_5-$ alkyl chains, which probably explains the observed thickness reduction. The developments of this parameter in Figure 5a and the dose dependence of the sulfur species amount in the upper level in Figure 5b are very similar at first sight. However, the observed thickness reduction noticeably exceeds the values expected for the solely desorption of the $CH_3(CH_2)_5-$ or $CH_3(CH_2)_5S-$ fragments (5.3 and 7.1 Å, respectively). Also the more precise model (thin solid line in Figure 5a) considering exclusively the determined reduction of the sulfur species in the upper level (Figure 5b) and the respective desorption of the $CH_3(CH_2)_5S-$ fragments does not reproduce the observed thickness reduction vs dose dependence for the HMUT film. As seen in Figure 5a, the difference of the thickness reduction in the strongly irradiated HMUT and C12/C18 films is ≈2.1 Å. This value makes up only ≈35% of the respective value in the latter films (≈6.1 Å). Consequently, the major thickness decrease in HMUT/Au is still related to the cleavage of the C−C bonds in its upper part as this happens in the C12/C18 films.[11] The occurrence of the C−S bonds (upper sulfur level) which are obviously more sensitive to electron irradiation than the C−C ones just increases the probability of bond scissions and subsequent desorption events.

The different behavior of sulfur in the lower and upper levels is also illustrated by Figure 5c. There the normalized ratios of the entire C 1s XPS intensity to the S 2p XPS intensities related to the lower (filled down triangles) and upper (filled up triangles) sulfur levels are presented. Whereas C_{tot}/S_{upper} increases with the progressive irradiation, C_{tot}/S_{lower} decreases to ≈42% of its initial value. Considering that the bonding energy of the C−S bond (≈66 kcal/mol) is larger than that of thiolate−Au bond (≈44 kcal/mol[12]) the major difference between sulfide and thiolate must lie in their position with respect to the Au substrate. Two factors seem to be of importance. First, a dipole−dipole coupling of the electronically excited state with its image at the metal can result in a quenching of this state, with the probability for this process reducing with increasing separation from the metal surface.[4,9] Second, a trapping of the sulfur-containing fragments in the alkyl matrix can occur, with the probability for this process reducing with decreasing distance to the film surface. Such a trapping can be mediated both by van der Waals interaction and by the bonding of the cut off fragments to one of the irradiation-induced radicals in the damaged alkyl matrix.

In this relation, the coincidence of the bonding energies of the sulfide species in the pristine HMUT film and irradiation-induced sulfur species in AT SAMs have to be considered. It is generally believed that the latter species are disulfides,[2,3] which is supported by the coincidence of the respective BE with that for sulfur in diaminodiphenyl and dialkyl disulfides[3,47] and by a predominant dialkyl disulfide desorption at heating of AT SAMs.[48−50] However, thermo- and electron-stimulated desorption may result in essentially different desorption fragments and the BE of the irradiation-induced sulfur species also coincides with that of alkyl sulfide. Thus, along with the disulfide formation the incorporation of sulfur into the alkyl matrix via bonding to irradiation-induced carbon radicals in the adjacent aliphatic chains is in principle possible, as it was recently noticed in ref 4. It should be noted, however, that the irradiation-induced sulfur species evolving into the double-bond cross-linking were not observed in the conventional AT SAMs, which is probably related to a low sulfur concentration in the surface region where the majority of the irradiation-induced events occurs. Alternatively, the sulfide-derived sulfur species in the irradiated HMUT film should be located on the residual film surface. The occurrence of these species in the surface region can provide an additional cross-linking which can probably slow down the irradiation-induced damage of the residual film. This might be the reason for the lower rates of the NEXAFS resonances and anisotropy maxima reduction in the respective spectra as compared to C12/C18 and for the observed difference of the C_{tot}/S_{lower} ratio in the irradiated HMUT film and the C_{tot}/S ratio in irradiated C18 (see the dashed line in Figure 5c).

5. Conclusion

The structure of SAMs formed from 11-(hexylmercapto)-undecane-1-thiol on gold, and their modification by low-energy electrons, were investigated by XPS and NEXAFS spectroscopy. It has been found that HMUT forms a dense, well-ordered self-assembled monolayer on Au with a coverage close to that of alkanethiolate SAMs, a thickness of 19.8 ± 0.5 Å, and an average tilt angle of the individual molecules of 40° ± 2°. Features related to thiolate and sulfide can be easily distinguished in S 2p XP spectra.

The electron irradiation of HMUT/Au gives rise to similar effects previously observed for AT SAMs. Some differences are, however, perceived. First, the extent of the irradiation-induced desorption in HMUT is found to be noticeably larger (by more than 35%), which is attributed to a higher sensitivity of C−S bond to electron irradiation as compared to C−C ones. Nevertheless, the majority of desorption events is believed to be related to C−C bond scission in the same way as this happens in AT SAMs. Second, an irradiation-induced, sulfide-derived sulfur species presumably involving into C═S double bonding were detected. Third, an extent of the irradiation-induced damage in the residual HMUT film and on Au-thiolate interface is slightly reduced, which is believed to be related to an additional cross-linking mediated by a sulfide-derived sulfur species.

A close resemblance of the binding energies of the alkyl sulfide and the irradiation-induced sulfur species in AT SAM implies an alternative assignment for the latter species along with a commonly approved disulfide formation model, namely an incorporation of sulfur into the alkyl matrix via bonding to irradiation-induced carbon radicals in the adjacent aliphatic chains. XPS measurements with a high energy resolution or TOF SIMS experiments are of interest to distinguish between these two possible scenarios.

From the point of view of the possible lithographic applications the incorporation of the specific molecular groups and, in particular, a sulfide entity into the alkyl matrix seems to be a prospective way to increase the sensitivity of the AT SAMs with respect to electron, X-ray, or ion irradiation. Otherwise, such groups can be used and considered as a microscopic sensor providing us with a location specific information. Considering the obtained experimental results in this way, we find strong support for the previous determinations[4,9,11] concerning a predominant location of the irradiation-induced bond scission events in the topmost part of the AT SAMs.

Acknowledgment. We thank the BESSY staff, especially M. Mast, for technical help during some stages of the experiments, G. Albert for the preparation of the gold substrates, and Prof. Ch. Wöll (Universität Bochum) for providing us with experimental equipment. We are also very obliged to Prof. M. Grunze for useful discussions. This work has been supported by the German Bundesministerium für Bildung, Wissenschaft, Forschung und Technologie (BMBF) through grants No. 05 SF8VHA 1, 05 SL8VHA 2, and 13N7167 and by the Fonds der Chemischen Industrie. A.U. thanks the NSF for funding through the MRSEC for Polymers at Engineered Interfaces.

References and Notes

(1) Ulman, *An Introduction to Ultrathin Organic Films: Langmuir−Blodgett to Self-Assembly*; Academic Press: New York, 1991; *Chem. Rev.* **1996**, *96*, 1533.

(2) Jäger, B.; Schürmann, H.; Müller, H. U.; Himmel, H.-J.; Neumann, M.; Grunze, M.; Wöll, Ch. *Z. Phys. Chem.* **1997**, *202*, 263.

(3) Wirde, M.; Gelius, U.; Dunbar, T.; Allara, D. L. *Nucl. Instrum. Methods Phys. Res. B* **1997**, *131*, 245.

(4) Zharnikov, M.; Geyer, W.; Gölzhäuser, A.; Frey, S.; Grunze, M. *Phys. Chem. Chem. Phys*. **1999**, *1*, 3163.

(5) Lercel, M. J.; Redinbo, G. F.; Craighead, H. G.; Sheen, C. W.; Allara, D. L. *Appl. Phys. Lett.* **1994**, *65*, 974.

(6) Müller, H. U.; David, C.; Völkel, B.; Grunze, M. *J. Vac. Sci. Technol. B* **1995**, *13*, 2846.

(7) Calvert, J. M. *J. Vac. Sci. Technol. B* **1993**, *11*, 2155.

(8) Bard, A.; Berggren, K. K.; Wilbur, J. L.; Gillaspy, J. D.; Rolston, S. L.; McClelland, J. J.; Phillips, W. D.; Prentiss, M.; Whitesides; G. M. *J. Vac. Sci. Technol. B* **1997**, *15*, 1805.

(9) Olsen, C.; Rowntree, P. A. *J. Chem. Phys.* **1998**, *108*, 3750.

(10) Müller, H. U.; Zharnikov, M.; Völkel, B.; Schertel, A.; Harder, P.; Grunze, M. J. *Phys. Chem. B* **1998**, *102*, 7949.

(11) Zharnikov, M.; Frey, S.; Heister, K.; Grunze, M. *Langmuir*, in press.

(12) Sellers, H.; Ulman, A.; Shnidman, Y.; Eilers, J. E. *J. Am. Chem. Soc.* **1993**, *115*, 9389.

(13) Ulman, A., Ed. *Thin films: self-assembled monolayers of thiols*; Academic Press: San Diego, CA, 1998.

(14) Dubois, L. H.; Nuzzo, R. G. *Annu. Rev. Phys. Chem.* **1992**, *43*, 437.

(15) Fenter, P.; Eberhardt, A.; Eisenberger, P. *Science* **1994**, *266*, 1216; Fenter, P.; Eberhardt, A.; Liang, K. S.; Eisenberger, P. *J. Chem. Phys.* **1997**, *106*, 1600. Fenter, P.; Schreiber, F.; Berman, L.; Scoles, G.; Eisenberger, P.; Bedzyk, M. J. *Surf. Sci.* **1998**, *412/413*, 213.

(16) Kondoh, H.; Nozoye; H. *J. Phys. Chem. B* **1998**, *102*, 2367.

(17) Schaible, M.; Petersen, H.; Braun, W.; Koch, E. E. *Rev. Sci. Instrum.* **1989**, *60*, 2172.

(18) Bernstorff, S.; Braun, W.; Mast, M.; Peatman, W.; Schröder, T. *Rev. Sci. Instrum.* **1989**, *60*, 2097.

(19) Stöhr, J. *NEXAFS Spectroscopy*; Springer: Berlin, 1996.

(20) Batson, P. E. *Phys. Rev. B* **1993**, *48*, 2608.

(21) Moulder, J. F.; Stickle, W. E.; Sobol, P. E.; Bomben, K. D. *Handbook of X-ray Photoelectron Spectroscopy*; Perkin-Elmer Corp.: New York, 1992.

(22) Frey, S.; Heister, K.; Tamada, K.; Zharnikov, M.; Grunze, M., manuscript in preparation.

(23) Shirley, D. A. *Phys. Rev. B* **1972**, *5*, 4709.

(24) Wertheim, G. K.; Butler, M. A.; West, K. W.; Buchanan, D. N. E. *Rev. Sci. Instrum.* **1974**, *45*, 1369.

(25) Hähner, G.; Kinzler, M.; Thümmler, C.; Wöll, Ch.; Grunze, M. *J. Vac. Sci. Technol. A* **1992**, *10*, 2758.

(26) Kinzler, M.; Schertel, A.; Hähner, G.; Wöll, Ch.; Grunze, M.; Albrecht, H.; Holzhüter, G.; Gerber, Th. *J. Chem. Phys.* **1994**, *100*, 7722.

(27) Dannenberger, O.; Weiss, K.; Himmel, H.-J.; Jäger, B.; Buck, M.; Wöll, Ch. *Thin Solid Films* **1997**, *307*, 183.

(28) Outka, D. A.; Stöhr, J.; Rabe, J. P.; Swalen, J. D.; *J. Chem. Phys.* **1988**, *88*, 4076.

(29) Hähner, G.; Kinzler, M.; Wöll, Ch.; Grunze, M.; Scheller, M.; Cederbaum, L. S. *Phys. Rev. Lett.* **1991**, *67*, 851; *Phys. Rev. Lett.* **1992**, *69*, 694 (erratum).

(30) Bagus, P. S.; Weiss, K.; Schertel, A.; Wöll, Ch.; Braun, W.; Hellwig, H.; Jung, C. *Chem. Phys. Lett.* **1996**, *248*, 129.

(31) Väterlein, P.; Fink, R.; Umbach, E.; Wurth, W. *J. Phys. Chem.* **1998**, *108*, 3313.

(32) Biebuyck, H. A.; Bain, C. D.; Whitesides, G. M. *Langmuir* **1994**, *10*, 1825.

(33) Laibinis, P. E.; Bain, C. D.; Whitesides, G. W. *J. Phys. Chem.* **1991**, *95*, 7017.

(34) Harder, P.; Grunze, M.; Dahint, R.; Whitesides, G. M.; Laibinis, P. E. *J. Phys. Chem. B* **1998**, *102*, 426.

(35) Thome, J.; Himmelhaus, M.; Zharnikov, M.; Grunze, M. *Langmuir* **1998**, *14*, 7435.

(36) Abrahamsson, S.; Larsson, G.; von Sydlow, E. *Acta Crystallogr.* **1960**, *13*, 770.

(37) Weast, R. C. *Handbook of Chemistry and Physics*; CRC Press: Boca Raton, FL, 1968.

(38) Burkert, U.; Allinger, N. L. *Molecular Mechanics*; American Chemical Society: Washington, DC, 1982.

(39) Clark, T. *Computational Chemistry*; Wiley: New York, 1985.

(40) Porter, M. D.; Bright, T.; Allara, D. L.; Chidsey, C. E. D. *J. Am. Chem. Soc.* **1987**, *109*, 3559.

(41) Nuzzo, R. G.; Fusco, F. A.; Allara, D. L. *J. Am. Chem. Soc.* **1987**, *109*, 2358.

(42) Bain, C. D.; Biebuyck, H. A.; Whitesides, G. M. *Langmuir* **1989**, *5*, 723.

(43) Walczak, M. W.; Chung, C.; Stole, S. M.; Widrig, C. A.; Porter, M. D. *J. Am. Chem. Soc.* **1991**, *113*, 2370.

(44) Rieley, H.; Kendall, G. K.; Zemicael, F. W.; Smith, T. L.; Yang, S. *Langmuir* **1998**, *14*, 5147.

(45) Bierbaum, K.; Kinzler, M.; Wöll, Ch.; Grunze, M.; Hähner, G.; Heid, S.; Effenberger, F. *Langmuir* **1995**, *11*, 512.

(46) Witte, G.; Weiss, K.; Jakob, P.; Braun, J.; Kostov, K. L.; Woell, Ch. *Phys. Rev. Lett.* **1998**, *80*, 121.

(47) Gölzhäuser, A.; Panov, S.; Schertel, A.; Mast, M.; Wöll, Ch.; Grunze, M. *Surf. Sci.* **1995**, *334*, 235.

(48) Nuzzo, R. G.; Zegarski, B. R.; Dubois, L. H. *J. Am. Chem. Soc.* **1987**, *109*, 733.

(49) Nishida, N.; Hara, M.; Sasabe, H.; Knoll. W. *Jpn. J. Appl. Phys.* **1996**, *35*, L799.

(50) Kondoh, H.; Kodama, C.; Nozoye, H. *J. Phys. Chem. B* **1998**, *102*, 2310.